chemical results in Table III, runs 1 and 2 vs run 3, show that benzoic acid must play a second role, besides as a proton source in the electrochemical formation (reaction 2) of H_2O_2, by either promoting the formation of the oxo porphyrin (reaction 3) or the epoxidation rate or oxo-porphyrin-olefin complex stability (reaction 4). Similar effects of acid-base combinations (buffers) have been reported in iron porphyrin-hydrogen peroxide reactions.[22a] Porphyrin degradation is extensive in the absence of the acid, and benzoate alone, as potential axial ligand, is insufficient (run 2).

Finally, we consider the epoxide yield and porphyrin stability results in Table VI, where the "protected" porphyrins are compared to [Mn(TPP)Cl]. As expected, these porphyrins were more resistant to degradation when used at low concentrations. Some decomposition does occur, however. It is noteworthy that [Mn(TF_5PP)Cl] gives a much higher yield at a low catalyst concentration than other porphyrins. This means a fast reaction step (4), which is consistent with high turnovers of F-substituted derivatives of manganese and iron tetraphenylporphyrin.[29] In addition, the faradaic efficiency of the electrolysis was lower with the protected porphyrins than with [Mn(TPP)Cl]. It may be that the competing catalase reaction (1) is more important for these materials.

Acknowledgment. This research was supported in part by grants from the NSF (R.W.M.) and NIH (J.P.C., Grant 5 RO1 GM17880). H.N. expresses gratitude for sabbatical leave support from the Yozaki Memorial Foundation for Science and Technology and from Keio University, Yokohama, Japan.

(29) Takagi, S.; Takahashi, E.; Miyamoto, T. K.; Sasaki, Y. *Chem. Lett.* **1986**, 1275.

Contribution from the Departments of Chemistry, Rensselaer Polytechnic Institute, Troy, New York 12180, and The University of North Carolina at Chapel Hill, Chapel Hill, North Carolina 27599-3290

Electrocatalytic Olefin Epoxidation Using Manganese Schiff-Base Complexes and Dioxygen

Colin P. Horwitz,*[1,2] Stephen E. Creager,[3] and Royce W. Murray*[3]

Received February 14, 1989

Electrochemical reduction of $[Mn^{III}(salen)]^+$ (salen = *N,N'*-ethylenebis(salicylaldiminato)) complexes in acetonitrile solution in the presence of benzoic anhydride, 1-methylimidazole, dioxygen, and an olefin yields the epoxide of the olefin in as much as 48% yield based on electrochemical charge passed. Cyclic voltammetric and rotating-disk voltammetric results are consistent with an electron/dioxygen bonding/electron (ECE) reaction sequence to produce a manganese-peroxo complex in which the O-O bond is subsequently heterolyzed by reaction with benzoic anhydride to yield a Mn(V)-oxo complex. Cis/trans kinetic competition experiments with *cis*-cyclooctene and *trans*-2-octene give a cis/trans reactivity ratio of 10 for the electrolytic epoxidation. Iodosylbenzene gives a ratio of 14 under comparable conditions. Electrolysis in the presence of cyclohexene yields primarily cyclohexene oxide and significant quantities of the allylic oxidation products 2-cyclohexen-1-one and 2-cyclohexen-1-ol.

The homogeneous catalytic transformation of organic substrates by transition-metal compounds is an area of intense research activity. This interest arises from the possibilities of improving existing or discovering new catalytic reactions and from the biological relevance of transition-metal compounds to active sites of various enzymes. There is also interest in using electrochemical techniques[4] in conjunction with metal complex catalysts. We recently used[5] a manganese porphyrin as an electrocatalyst in the reductive activation of dioxygen toward olefin epoxidation in a scheme considered as a model reaction for the cytochrome P450 class of monooxygenase enzymes

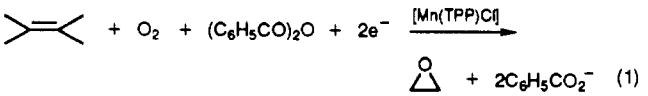

(1)

where Mn(TPP) is manganese(III) tetraphenylporphyrin and $(C_6H_5CO)_2O$ is benzoic anhydride.

Olefin epoxidation reactions have been extensively investigated[6] with manganese porphyrin catalysts, in which an activated form of oxygen, such as iodosylbenzene, is employed as the oxygen source (eq 2). The analogous reaction with manganese Schiff-base

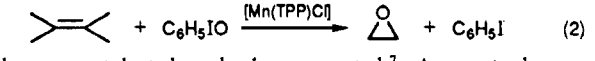

(2)

complexes as catalysts has also been reported.[7] A recent advance in this area[8] is olefin epoxidation using nickel Schiff-base and related complexes under phase-transfer conditions with NaOCl as the oxygen source. The nickel complexes are poor epoxidation catalysts when iodosylbenzene replaces hypochlorite.[8,9]

The necessity for the "preactivation" of dioxygen in the form of iodosylbenzene or hypochlorite is a potential disadvantage

(1) Rensselaer Polytechnic Institute.
(2) Work done at The University of North Carolina at Chapel Hill.
(3) The University of North Carolina at Chapel Hill.
(4) (a) See for example: Steckhan, E. *Angew. Chem., Int. Ed. Engl.* **1986**, *25*, 683. (b) *Organic Electrochemistry*; Baizer, M. M.; Lund, H., Eds.; Marcel Dekker: New York, 1983. (c) Scheffold, R.; Rytz, G.; Walder, L.; Orlinski, R.; Chilmonczyk, Z. *Pure Appl. Chem.* **1983**, *55*, 1791. (d) Collman, J. P.; Denisevich, P.; Konai, Y.; Marrocco, E.; Koval, C.; Anson, F. C. *J. Am. Chem. Soc.* **1980**, *102*, 6027.
(5) Creager, S. E.; Raybuck, S. A.; Murray, R. W. *J. Am. Chem. Soc.* **1986**, *108*, 4225.
(6) (a) See for example: Tabushi, I. *Coord. Chem. Rev.* **1988**, *86*, 1. (b) Castellino, A. J.; Bruice, T. C. *J. Am. Chem. Soc.* **1988**, *110*, 158. (c) Groves, J. T.; Stern, M. K. *Ibid.* **1987**, *109*, 3812. (d) Groves, J. T.; Watanabe, Y.; McMurry, T. J. *Ibid.* **1983**, *105*, 4489. (e) Collman, J. P.; Brauman, J. I.; Meunier, B.; Hayashi, T.; Kodadek, T.; Raybuck, S. A. *Ibid.* **1985**, *107*, 2000. (f) Smegal, J. A.; Schardt, B. C.; Hill, C. L. *Ibid.* **1983**, *105*, 3510. (g) Guilmet, E.; Meunier, B. *Tetrahedron Lett.* **1982**, 2449. (h) Carvalho, M. E.; Meunier, B. *Nouv. J. Chim.* **1986**, *10*, 39.
(7) (a) Srinivasan, K.; Michaud, P.; Kochi, J. K. *J. Am. Chem. Soc.* **1986**, *108*, 2309. (b) Dixit, P. S.; Srinivasan, K. *Inorg. Chem.* **1988**, *27*, 4507. (c) Srinivasan, K.; Perrier, S.; Kochi, J. K. *J. Mol. Catal.* **1986**, *36*, 297.
(8) (a) Yoon, H.; Burrows, C. J. *J. Am. Chem. Soc.* **1988**, *110*, 4087. (b) Kinneary, J. F.; Albert, J. S.; Burrows, C. J. *Ibid.* **1988**, *110*, 6124.
(9) Koola, J. D.; Kochi, J. K. *Inorg. Chem.* **1987**, *26*, 908.

0020-1669/90/1329-1006$02.50/0

compared to the direct reaction of dioxygen, which can be achieved electrochemically. We report here an electrocatalytic olefin epoxidation reaction utilizing [Mn^{III}(salen)][benzoate] or [Mn^{III}(salen)][Cl] (I) (salen = *N,N'*-ethylenebis(salicylaldiminato)) as

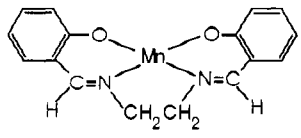

I

electrocatalysts in acetonitrile solvent. The results using these catalysts are compared and contrasted to our previous results[5] for the [Mn(TPP)Cl] catalyst.

Experimental Section

Materials. The Schiff-base compounds [Mn^{III}(salen)][benzoate], [Mn^{III}(salen)][Cl], and [Mn^{III}(salen)][PF_6] were prepared by using standard procedures.[7a,10] CH_3CN (Burdick and Jackson) and 1-methylimidazole (Aldrich) were dried over 5-Å sieves. *cis*-Cyclooctene, *trans*-2-octene, 2-cyclohexen-1-ol, and 2-cyclohexen-1-one (Aldrich) were used as received. Cyclohexene (Aldrich) was fractionally distilled prior to the epoxidation reaction, and purity was checked by GC analysis. Cyclooctene oxide and *trans*-2-octene oxide were prepared by reaction of the olefin with *m*-chloroperoxybenzoic acid. Benzoic anhydride was washed with aqueous bicarbonate to remove acids and then recrystallized from toluene/ethanol. Tetraethylammonium perchlorate, Et_4NClO_4, was prepared by using standard procedures, recrystallized three times from water, and dried at 50 °C in vacuo overnight.

Equipment and Electrochemistry. Cyclic voltammograms (CV) and rotating-disk-electrode (RDE) voltammograms were obtained in three-compartment electrochemical cells with locally built instrumentation and a Pt wire and an SSCE (sodium chloride saturated calomel electrode) as the auxiliary and reference electrodes, respectively. A Pine Instruments ASR-2 analytical rotator was used in the RDE experiments. The working electrode was a 0.1-cm^2 glassy-carbon disk, polished before each experiment with 1-μM diamond paste (Buehler). Acetonitrile solvent containing 0.1 M Et_4NClO_4 as the electrolyte was used throughout.

All electrochemical mixtures contained 1-methylimidazole as the postulated axial ligand unless otherwise indicated. The voltammetry was more reproducible when imidazole was present in solution, as it may act to prevent adsorption of the metal complex to the electrode.

Controlled-potential electrolyses (CPE) were conducted by using a Princeton Applied Research Model 173 potentiostat and Model 176 universal programmer. The data were obtained digitally with a Tecmar Labmaster 12-bit analog to digital interface in conjunction with an IBM-PC XT computer. CPE experiments were performed by using either a carbon flag (A = 7 cm^2) or a carbon crucible (A = 15 cm^2) as the working electrode. The counter electrode, a coiled Pt wire, was separated from the working solution by a fine-porosity frit, while the reference electrode, a SSCE, was placed directly in the working solution. An atmosphere of purified Ar or O_2 saturated with CH_3CN was maintained over the reaction mixture. Products were analyzed chromatographically with a Hewlett-Packard GC 5750 with 10% OV-101 on Chromosorb P as the stationary phase. Vis–UV spectra were taken on a Tracor-Northern 6051 diode-array spectrophotometer.

Results and Discussion

We will begin with a summary of our findings in order to facilitate discussing how these conclusions were obtained. The reaction pathway proposed from analysis of the chemical and electrochemical experiments is shown in Figure 1. Formal charges and metal oxidation states are assigned to the various species presented throughout the paper in order to simplify the following discussion, but these are not meant to be interpreted rigorously. Mechanistically, the epoxidation reaction is analogous to that presented[5] for the manganese porphyrin catalyst based system. The essential details are the binding of O_2 to the Mn(II) center formed by one-electron electrochemical reduction of the Mn(III) complex, followed by the transfer of a second electron to form what formally can be written as a Mn(III)–peroxo complex. The three steps involved in the O_2-activation process represents a classical EC_iE (E = electron transfer and C = chemical reaction)

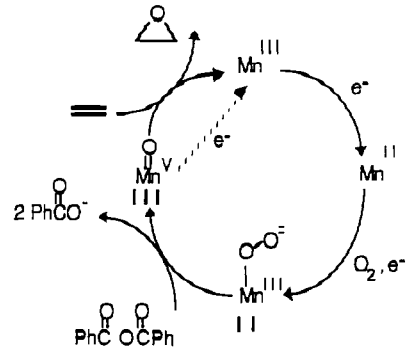

Figure 1. Proposed scheme for electrolytic epoxidation.

reaction sequence. A key step in the activation process is subsequent cleavage of the O–O bond by an electrophilic activator, in this instance benzoic anhydride. Conditions are sought, by using a large excess of olefin, such that once the Mn(V)–oxo species is formed, transfer of the oxygen to the olefin is relatively rapid.

The data presented first will be the results of electrolytic epoxidation experiments in which all the reactant ingredients of Figure 1 are present and the results obtained are in terms of GLC-analyzed reaction product and the efficiency of its production. We will then turn to cyclic voltammetry (CV), rotating-disk-electrode (RDE) voltammetry, and controlled-potential electrolysis (CPE) by which, manipulating the experimental time scale and the reagents present, we further probe the reaction scheme shown in Figure 1.

Electrolytic Epoxidation. A typical electrolysis reaction mixture included 0.5 mM [Mn^{III}(salen)][benzoate or chloride], 6 mM 1-methylimidazole, and 0.1 M each of Et_4NClO_4, olefin, and benzoic anhydride. The anhydride's function (Figure 1) is to cleave the O–O bond once the oxygen is coordinated to and activated by the metal center (eq 3). Controlled-potential

$$[Mn^{III}(salen)—O_2]^- + (C_6H_5CO)_2O \rightarrow [(salen)Mn{=}O] + 2[C_6H_5CO_2]^- \quad (3)$$

electrolyses were performed at −0.45 V vs SSCE by using either a carbon crucible or carbon flag as the working electrode. This potential is negative enough to reduce the [Mn^{III}(salen)]$^+$ complex but not negative enough to cause direct reduction of dioxygen in this medium. (The latter electrode reaction is undesirable, since it may (by using trace H_2O in the medium) lead to hydrogen peroxide and a second pathway for epoxidation like that explored for porphyrins by Mansuy.[11]) An atmosphere of dioxygen was maintained above the electrolysis solution to ensure a constant concentration of dissolved O_2 in the reaction medium. Each electrolysis mixture was preelectrolyzed for 15 min prior to addition of the [Mn^{III}(salen)]$^+$ catalyst to ascertain whether products could be formed in the absence of the catalyst, with negative results (by GLC analysis) in all cases.

The olefins, *cis*-cyclooctene, *trans*-2-octene, and cyclohexene, were chosen as model epoxidation substrates. The two octenes were used in kinetic competition experiments to probe the steric selectivity of the Schiff-base catalyst; this olefin pair has been previously exploited to probe relative cis/trans reactivities in related metalloporphyrin systems.[6e,12] The reaction of cyclohexene additionally explores possible allylic oxidation pathways; epoxide is formed from cyclohexene when concerted or nearly concerted transfer of an oxygen atom occurs (eq 4), whereas a radical, allylic oxidation pathway can generate[7a,13] 2-cyclohexen-1-ol and 2-

(10) Holm, R. H.; Everett, G. W.; Charkavorty, A. *Prog. Inorg. Chem.* **1966**, *7*, 82.

(11) (a) Renaud, J.-P.; Battoni, P.; Bartoli, J.-F.; Mansuy, D. *J. Chem. Soc., Chem. Commun.* **1985**, 888. (b) Mansuy, D.; Bartoli, J.-F.; Chottard, J.-C.; Lange, M. *Angew. Chem., Int. Ed. Engl.* **1980**, *19*, 909. (c) Mansuy, D.; Bartoli, J.-F.; Momenteau, M. *Tetrahedron Lett.* **1982**, *23*, 2781.

(12) Collman, J. P.; Brauman, J. I.; Meunier, B.; Raybuck, S. A.; Kodadek, T. *Proc. Natl. Acad. Sci. U.S.A.* **1984**, *81*, 3245.

(13) (a) Meunier, B.; Guilmet, E.; De Carvalho, M. E.; Poilblanc, R. *J. Am. Chem. Soc.* **1984**, *106*, 6668. (b) Powell, M. F.; Pai, E. F.; Bruice, T. C. *Ibid.* **1984**, *106*, 3277.

Table I. Olefin Epoxidation[a] with $[Mn^{III}(salen)][X]$ Catalysts (X = Benzoate (A), Chloride (B), PF_6^- (C))

catalyst (mM)	0.1 M olefin	product (mM)	Q_{eff}, %[b]	turnovers	cis/trans	oxo/allylic
		Electrolytic Oxidation				
B (0.59)	cyclooctene	cyclooctene oxide (1.4)	35	2.4		
B (0.5)	cyclooctene	cyclooctene oxide (0.98)	38	2	8	
	trans-2-octene	*trans*-2-octene oxide (0.12)				
A (0.45)	cyclooctene	cyclooctene oxide (0.7)	48	1.6		
A (0.45)	cyclooctene	cyclooctene oxide (0.75)	43	1.8	10	
	trans-2-octene	*trans*-2-octene oxide (0.07)				
A (0.6, 0.6)	cyclohexene	cyclohexene oxide (1.3, 2.1)[c]	90, 81[c]	3, 4[c]		2.4, 5.8[c]
		2-cyclohexen-1-ol (0.18, 0.2)[c]				
		2-cyclohexen-1-one (0.36, 0.16)[c]				
		Chemical Oxidation with Iodosylbenzene Oxidant				
A (0.41)	cyclooctene	cyclooctene oxide (2.5)	68	6	14	
	trans-2-octene	*trans*-2-octene oxide (0.18)				
C[d]	cyclohexene					13

[a] All solutions contain 6 mM 1-methylimidazole, 0.2 M Et_4NClO_4, and 0.1 M benzoic anhydride in CH_3CN. [b] Assuming a two-electron process in the electrochemical experiments and a 1:1 molar stoichiometry of PhIO/olefin in the PhIO results. [c] Results from two catalytic runs. [d] Reference 7a.

cyclohexen-1-one as in eq 5a or alternatively, as suggested by a reviewer, as in eq 5b.

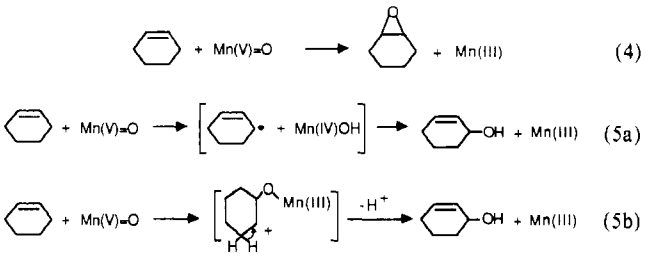

Table I presents the electrolytic epoxidation results. GLC product analyses for the olefin pair *cis*-cyclooctene and *trans*-2-octene (top entries) showed only unreacted olefin and the corresponding epoxides, as expected. The essential results for the olefin pair are that (i) epoxide is produced with reasonable efficiency (as much as 48% yield) of use of the electrochemical charge, (ii) the reaction is catalytic (>1 turnover of catalyst), and (iii) epoxidation of the cis isomer is strongly favored (ca. 10×) over the trans isomer. The last result is consistent with a preferred orientation for approach of the olefin to the presumed active oxidant III (Figure 1). On the other hand, the cis/trans reaction selectivity of both $[Mn^{III}(salen)]^+$ catalysts seems to be smaller than that (15:1) of the manganese tetraphenylporphyrin catalyst in an analogous electrolytic epoxidation.[14] Approach of the trans form of the olefin to the oxo form of the Schiff-base complex, III, is sterically less hindered due both to the probably more rigorously enforced square-planar nature of the manganese center in the porphyrin oxo form ((TPP)Mn=O) and to its phenyl substituents.

The catalytic efficiency in Table I, Q_{eff}, is expressed as the ratio of moles of epoxide product analyzed to the electrochemical charge passed (expressed in moles, assuming a two-electron reaction; see Figure 1). Both the catalytic efficiency and the cis/trans reaction selectivity of the two complexes are somewhat larger for the benzoate form of the $[Mn^{III}(salen)]^+$ complex as compared to the chloride form, but the difference is not large.

A comparison, chemical oxidation ("shunt") vs electrochemical oxidation for the olefin pair *cis*-cyclooctene and *trans*-2-octene was performed by using iodosylbenzene as oxidant and $[Mn^{III}(salen)]$[benzoate] as catalyst and 0.1 M Et_4NClO_4/CH_3CN as solvent medium (Table I, lower entry). Both the cis/trans reaction selectivity and the catalytic efficiency (in this case using moles of oxidant) were somewhat higher than in the electrochemical experiment, but again the differences are not large. The difference in catalytic efficiency is explicable on the basis of possible electrochemical consumption of the active oxidant III, as indicated by the dashed arrow ("short-circuit reaction") in Figure 1 (vide infra). The iodosylbenzene oxidation results (both catalytic efficiency and cis/trans selectivity) in Table I were independent of whether benzoic anhydride was present or not, so the course of the reaction following generation of III appears to be the same whether III is generated electrochemically or chemically.

Appreciable quantities of allylic oxidation products, 2-cyclohexen-1-one and 2-cyclohexen-1-ol, are observed with cyclohexene as olefin substrate in the electrolytic epoxidation (Table I). The ketone is likely a secondary dioxygen oxidation product of the alcohol.[15] Detection of the allylic oxidation products strongly suggests that, to some extent, the oxidation reaction proceeds along either the radical pathway eq 5a or the stepwise cationic mechanism eq 5b, at least for cyclohexene. Allylic oxidation of cyclohexene also occurs for the manganese porphyrin catalyst, producing a similar ratio of epoxide/allylic oxidation products.

Catalytic iodosylbenzene-based epoxidation of cyclohexene with $[Mn^{III}(salen)][PF_6]$ as catalyst was reported by Kochi et al.[7] to generate significant yields of cyclohexene oxide but only trace quantities of 2-cyclohexen-1-ol and no 2-cyclohexen-1-one (Table I, last entry). It is not clear what aspect of the electrochemical reaction drives its greater incidence of allylic oxidation products. The addition of water (0.5 vol %) to the electrolysis mixture did not affect our electrochemical result, so traces of benzoic acid formed from the anhydride are not significant. We were not successful in exploring the possible influence of the acid anhydride electrophile by using alternative acid anhydrides; succinic anhydride had an unexplained adverse effect on the $[Mn^{III/II}(salen)]^{+/0}$ electrochemistry even in the absence of oxygen or olefins. It is perhaps notable that the electrochemical system includes at least one reaction intermediate that the chemical oxidation system does not, the peroxo-Mn(III) complex II (Figure 1), that might initiate a radical pathway.

Cyclic Voltammetry. As we have shown before[16] for $[Mn(TPP)]^+$, cyclic voltammetry and rotated-disk-electrode voltammetry are useful in exploring the action of the $[Mn^{III}(salen)]^+$ catalyst in inducing electrochemical reduction of dioxygen and the electroactivity of the *oxo* form of the catalyst. The essential idea is to compare the electrochemical behavior of the metal complex alone, in combination with dioxygen, and in combination with dioxygen plus benzoic anhydride. It must be appreciated in doing this that cyclic voltammetry explores the behavior of these reaction step components of Figure 1 on a faster time scale than does an electrolytic epoxidation experiment.

Addition of Dioxygen. Cyclic voltammetry of $[Mn^{III}(salen)]$[benzoate] in the absence (Ar atmosphere) of dioxygen (Figure 2) shows a diffusion-controlled ($i_p \propto v^{1/2}$), quasi-reversible (E_p = 110 mV) wave for the $[Mn^{III/II}(salen)]^{+/0}$ couple at $E°$ = −275 mV vs SSCE. The changes that occur upon admission of O_2 are (i) enhancement of the reduction current at the (un-

(14) Creager, S. E. Ph.D. Thesis, The University of North Carolina at Chapel Hill, 1987.

(15) Groves, J. T.; Nemo, T. E. *J. Am. Chem. Soc.* **1983**, *105*, 5791.
(16) Creager, S. E.; Murray, R. W. *Inorg. Chem.* **1987**, *26*, 2613.

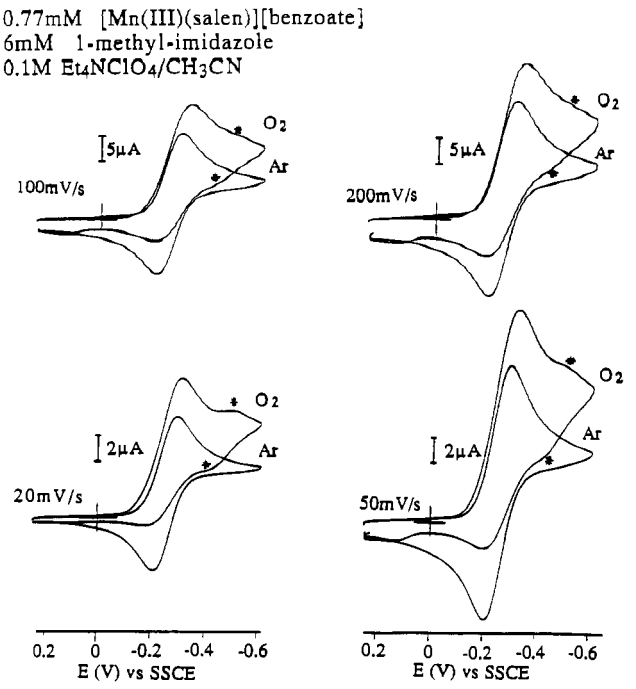

Figure 2. Cyclic voltammetry at a glassy-carbon electrode, with conditions as indicated on the diagram, under Ar and under O_2.

changed) potential for the $[Mn^{III/II}(salen)]^{+/0}$ reaction, (ii) diminution of the corresponding current for oxidation of $[Mn^{II}(salen)]$, and (iii) appearance of a small wave (see the asterisk) at more negative potential, ca. −450 mV (vide infra).

Enhancement of the $[Mn^{III/II}(salen)]^{+/0}$ reduction current, and diminution of the corresponding $[Mn^{II/III}(salen)]^{0/+}$ oxidation current, are the results expected for binding of dioxygen to $[Mn^{II}(salen)]$ followed by passage of a second electron to the (thermodynamically) even more easily reduced dioxygen adduct, forming $[Mn^{III}(salen)-O_2]^-$. The effect is parallel to the ECE sequence observed for the $[Mn(TPP)]^+$ system.[16] If the $[Mn^{II}(salen)]$–dioxygen binding constant is large and the binding reaction is fast, the $[Mn^{III/II}(salen)]^{+/0}$ reduction current ideally should be enhanced 2.8 times.[17] Figure 2 shows (see also data in Table II) that the effect is about half that, 1.4 times. Both the enhancement of the reduction current and the diminution of $[Mn^{II/III}(salen)]^{0/+}$ oxidation current are furthermore lessened at the faster potential scan rates, which suggests that a kinetic effect is at least in part responsible. The occurrence of the more negative voltammetric process (*) in Figure 2 complicates cyclic voltammetric consideration of the kinetics, however, since we believe this process to be a major sink for the dioxygen adduct intermediate, $[Mn^{III}(salen)-O_2]^-$, as discussed next.

We believe that the wave at more negative potentials (ca. −450 mV vs SSCE; asterisk in Figure 2) reflects formation of a dimeric species in the presence of dioxygen. Dimer formation in the reaction of $[Mn^{III}(salen)][PF_6]$ with iodosylbenzene has been postulated,[7] and manganese Schiff-base complexes are known[18] to form oxo- or dioxo-bridged species in the presence of dioxygen, by reactions such as eqs 6–8. Note that, as the potential is scanned

$$[Mn^{III}-O_2]^- + [Mn^{II}] \rightarrow [Mn^{III}-O_2-Mn^{III}]^- \quad (6)$$

$$[Mn^{III}-O_2]^- + [Mn^{III}]^+ \rightarrow [Mn^{III}-O_2-Mn^{IV}] \quad (7)$$

$$2[Mn^{III}]^+ + O_2 \rightarrow [Mn^{IV}-O_2-Mn^{IV}]^{2+} \quad (8)$$

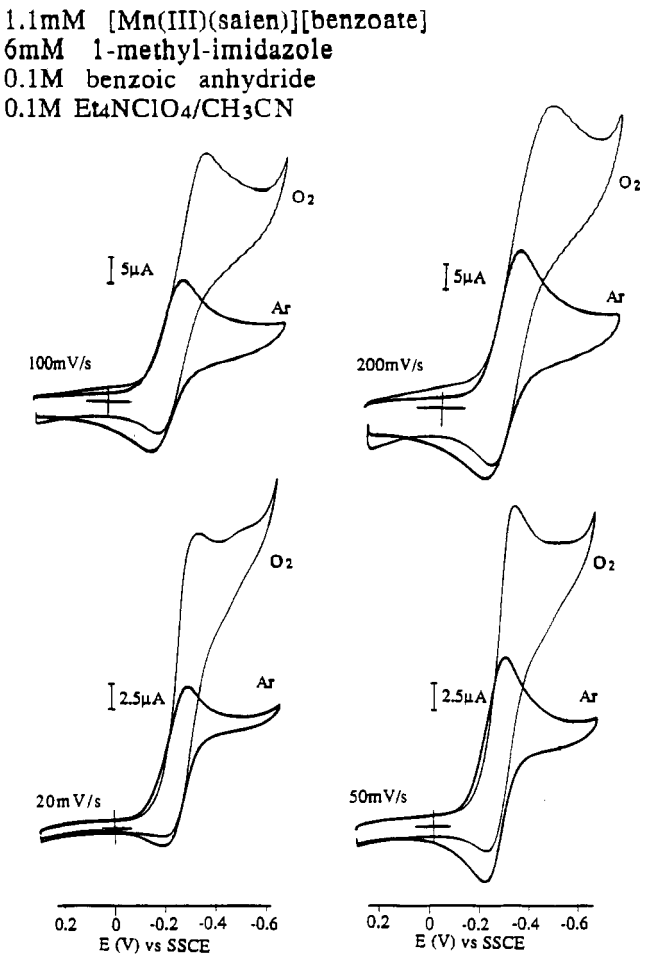

Figure 3. Cyclic voltammetry at a glassy-carbon electrode, with conditions as indicated on the diagram, under Ar and under O_2.

through the $[Mn^{III/II}(salen)]^{+/0}$ wave, $[Mn^{III}(salen)]^+$, $[Mn^{II}(salen)]$, and $[Mn^{III}(salen)-O_2]^-$ complexes coexist in the diffusion layer around the electrode. Dimer formation is consistent with the smaller size of the −450-mV (*) wave (relative to the $[Mn^{III/II}(salen)]^{+/0}$ wave) that is observed in cyclic voltammetry when lower concentrations of the Schiff-base complex are used (a more dilute diffusion layer) and faster potential scan rates are used (Figure 2; the asterisk wave is quite faint at 200 mV/s), where smaller quantities of the dioxygen adduct $[Mn^{III}(salen)-O_2]^-$ have been formed. The primary point to be made is that dimer formation, whether by eq 6 or 7, would act to prevent passage of a second electron to the dioxygen adduct $[Mn^{III}(salen)-O_2]^-$ and thus serve to depress the extent to which current enhancement could occur at the potential of the $[Mn^{III/II}(salen)]^{+/0}$ wave.

The more negative dimer wave was *not* observed in the rotating-disk voltammetric experiments discussed below. This strongly implicates eq 7 as the primary dimer-forming reaction, on the basis of consideration[19] of the differing compositions of the diffusion layers around electrodes whose potential is scanned rapidly (as in cyclic voltammetry) versus very slowly (as in the pseudo-steady-state conditions of rotated disks). Concurrently, an essentially complete two-electron reduction is observed by rotated-disk voltammetry for the $[Mn^{III}(salen)]^+$ complex in the presence of dioxygen.

Finally, we should note that appreciable currents arising from direct reduction of dioxygen do not begin until ca. −0.8 V, a much

(17) Cyclic voltammetric peak currents are ideally proportional to the number of electrons transferred to the $^3/_2$ power; $2.8 = 2^{3/2}$.

(18) (a) Fredrick, F. C.; Taylor, L. T. *Polyhedron* **1986**, *5*, 887. (b) Sawodny, W.; Grunes, R.; Reitzle, H. *Angew. Chem., Int. Ed. Engl.* **1982**, *21*, 775. (c) Maslen, H. S.; Waters, T. W. *J. Chem. Soc., Chem. Commun.* **1973**, 760. (d) Miller, J. D.; Oliver, F. D. *J. Inorg. Nucl. Chem.* **1972**, *34*, 1873. (e) Matsushita, T.; Yarino, T.; Masuda, I.; Shono, T.; Shinra, K. *Bull. Chem. Soc. Jpn.* **1973**, *46*, 1712. (f) Boucher, L. J.; Coe, C. G. *Inorg. Chem.* **1975**, *14*, 1289.

(19) In cyclic voltammetry, appreciable amounts of the $[Mn^{III}(salen)-O_2]^-$ and $[Mn^{III}(salen)]^+$ complexes intermingle in the diffusion layer around the electrode as the potential is gradually scanned through the $[Mn^{III/II}(salen)]^{+/0}$ wave, allowing opportunity for eq 7. In rotating-disk voltammetry, at a potential on the limiting current for $[Mn^{III}(salen)]^+$ reduction, the population of the $[Mn^{III}(salen)]^+$ complex is *zero* at the electrode/solution interface and correspondingly is much less throughout the diffusion layer, so an eq 7 reaction is less feasible.

Table II. Electrochemical Data[a]

compd	E°, mV[b]	E_p, mV	$i_{p,O_2}/i_{p,Ar}$ 20 mV/s	50 mV/s	100 mV/s	200 mV/s
Mn(salen)benz[c]	−260	110	1.4	1.4	1.3	1.2
Mn(salen)benz[c,d]	−240	120	2.8	2.6	2.3	1.9
Mn(salen)Cl[c]	−250	140	1.8	2.3	3.6	3.7

[a] CH_3CN, 0.1 M Et_4NClO_4 vs SSCE. [b] Ar atmosphere. [c] 1-Methylimidazole (6 mM). benz = benzoate. [d] Benzoic anhydride (0.1 M) present.

more negative potential than those of the reactions shown in Figure 2. This favorable situation, avoiding overlap with direct dioxygen reduction, is based on the choice of a glassy carbon as the working electrode; dioxygen electrode kinetics are slow on glassy carbon.

Addition of Dioxygen and Benzoic Anhydride. Cyclic voltammetry for [Mn^{III}(salen)][benzoate] in the presence of 0.1 M benzoic anhydride and under Ar (Figure 3) occurs at a somewhat more positive potential, −240 mV vs SSCE, and continues to be well defined.[20] Aerating the cell with dioxygen enhances the reduction current, much more than was observed in the absence of the acid anhydride (see Table II; compare first and second entries). This is the result expected if the doubly reduced dioxygen adduct [Mn^{III}(salen)−O_2]$^-$ can react with the acid anhydride (eq 3) at a rate comparable to the time scale with which the [Mn^{III}(salen)−O_2]$^-$ adduct can diffuse out of the diffusion layer around the electrode. Its reaction should produce the metal–oxo complex, which is expected to be reducible[21] at the potential required for the [$Mn^{III/II}$(salen)]$^{+/0}$ reaction. Reduction of the oxo form of the complex, indicated as the short-circuit reaction (dashed line) in Figure 1, is thus the source of the additional current in Figure 3 as compared to Figure 2. This is an important observation inasmuch as operation of the short-circuit reaction has the effect of lowering the efficiency of use of electrochemical equivalents in an electrolytic epoxidation, and electrochemical reduction of the oxo form may account for the less than 100% catalytic efficiencies observed in Table I. As we have discussed elsewhere,[16] however, the quantitative impact of the short-circuit reaction depends on a subtle interplay between the rate of the oxo-form generation and its consumption by olefin versus the rate of electrochemical mass transport, so relating catalytic efficiency in Table I to the enhanced currents of Figure 3 is easily done on a qualitative but not a quantitative level.

Chloride Complex. Cyclic voltammetry for the complex [Mn^{III}(salen)][Cl], under conditions like those in Figure 2, shows qualitatively similar, but larger (Table II), reduction current enhancements in the presence of dioxygen. There are a number of significant details that differ between the benzoate and chloride complexes, however. Apparently there is a rapid and/or irreversible dissociation of chloride from the reduced complex, the kinetics of which have a complex interplay with those of dioxygen binding and the potential scan and lead to dioxygen-based current enhancements that increase, rather than decrease, at fast potential scan rates. It is possible to rationalize these effects, but a much more detailed kinetic study is needed before presentation of an adequately defensible scheme.

Rotating-Disk-Electrode Voltammetry. Rotating-disk-electrode (RDE) voltammetry, largely because of the absence of dimer effects, gave better quantitation of the additional reduction current passed to the [Mn^{III}(salen)][benzoate] complex in the presence of dioxygen. Well-defined steady-state waves and limited currents were observed, which were measured as a function of the electrode rotation rate, w. According to the Levich equation,[23] a transport-limited current at a RDE is[24]

$$i_{lim} = 0.620nFAD_0^{1/2}w^{1/2}\nu^{-1/6}C_0^* \quad (9)$$

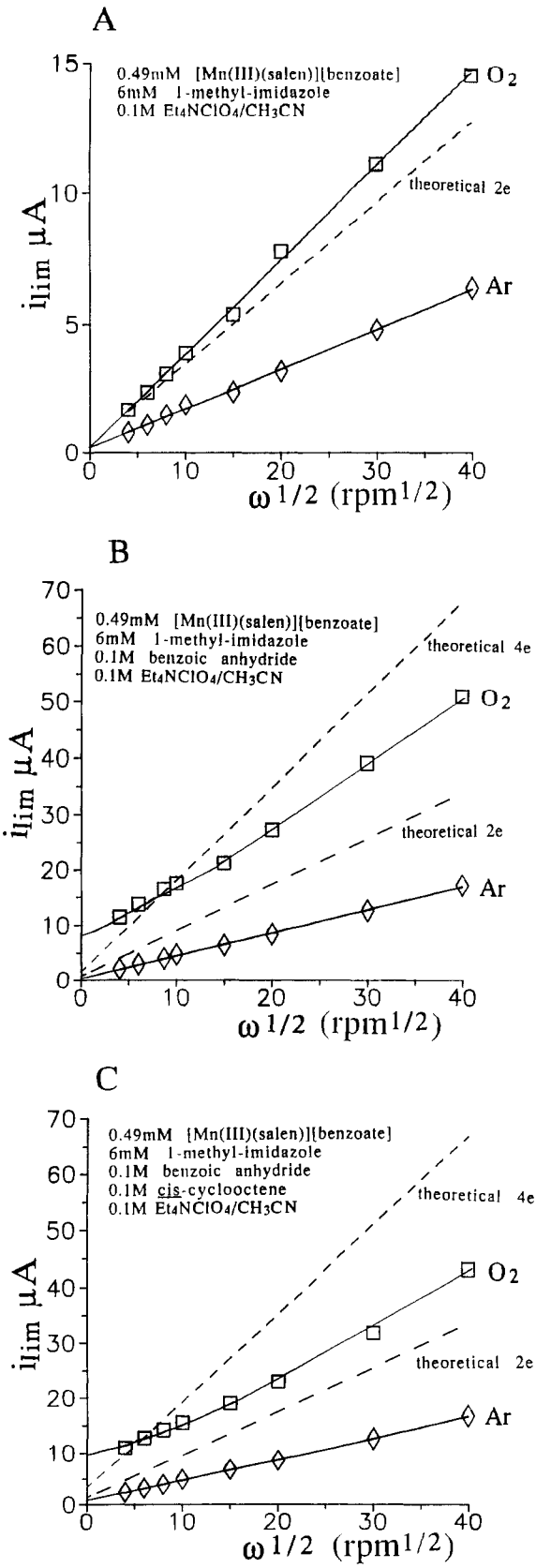

Figure 4. Levich plots of limiting currents, measured at −0.45 V vs SSCE. The theoretical lines for two- and four-electron processes are based on multiples of the n = 1 slope in panel A, under Ar.

(20) The currents observed in the presence of benzoic anhydride, under Ar, are above twice those observed in its absence, by both CV and RDE voltammetry. The reason(s) for this are not clear.

(21) Oxidations of Mn(IV)–oxo complexes to what are presumed to be the high-valent Mn(V)–oxo species are well documented.[6c,19] Thus, reduction of Mn(V)–oxo should also be feasible.

(22) Smegal, J. A.; Hill, C. L. *J. Am. Chem. Soc.* **1983**, *105*, 5791.

(23) Bard, A. J.; Faulkner, L. F. *Electrochemical Methods*; Wiley: New York, 1980.

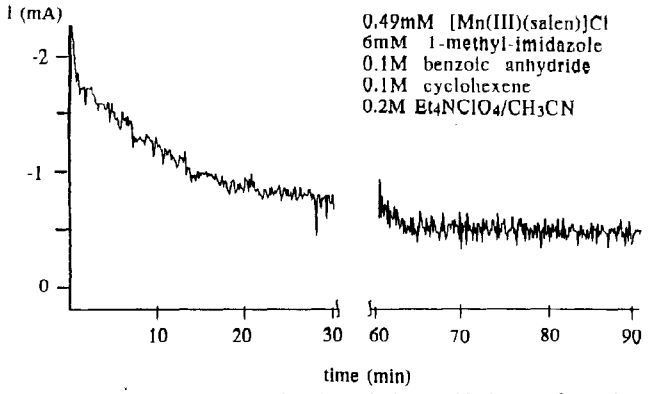

Figure 5. Current–time curve for electrolytic epoxidation, performed at −0.45 V vs SSCE.

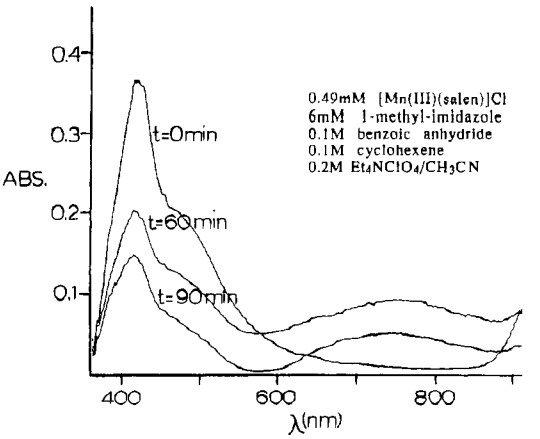

Figure 6. Spectra taken during the electrolysis shown in Figure 5, at indicated times.

The limiting current i_{lim} should vary with $w^{1/2}$ with a proportionality constant containing the number of electrons in the electrode reaction, n. Figure 4 shows how the limiting current measured at −0.45 V vs SSCE changes with rotation rate for solutions of $[Mn^{III}(salen)]^+$ with and without dioxygen (Figure 4A), with added benzoic anhydride (Figure 4B), and with added benzoic anhydride and cyclooctene (Figure 4C).

In the absence of dioxygen, i_{lim} vs $w^{1/2}$ plots (Levich plots) are linear, pass through the origin, and serve to establish the value of the proportionality constants in eq 9 for the one-electron $[Mn^{III/II}(salen)]^{+/0}$ reduction (Figure 4A). When dioxygen is added, if the $[Mn^{II}(salen)]$–dioxygen binding reaction occurs rapidly and completely on the time scale of transport through the hydrodynamic diffusion layer, a second electron will be passed to form the $[Mn^{III}(salen)–O_2]^-$ complex, and the slope of the Levich plots should be doubled (i.e., $n = 2$). As seen in Figure 4A, the experimental limiting currents fall reasonably close to the hypothetical two-electron line ($n_{app} = 2.3$).

Addition of benzoic anhydride (0.1 M) to the solution yields even larger reduction currents as was seen in the cyclic voltammetric results (Figure 3). The Levich plot shown in Figure 4B has a slope in the presence of O_2 that is approximately 2.6 times (n_{app}) greater than that in an Ar atmosphere. This means that eq 3, producing the electroreducible oxo complex, occurs to a significant extent (but not quantitatively)[25] on the time scale of residence of the doubly reduced $[Mn^{III}(salen)–O_2]^-$ within the diffusion layer. Significantly, the experimental Levich line begins to flatten out at low electrode rotation rate. There, we see i_{lim} values *above* the four-electron slope, clearly leading to a nonzero current intercept. This is behavior expected for an *electrocatalytic* current in which the manganese catalyst effects a four-electron reduction of dioxygen using benzoic anhydride as the electrophile.

Inclusion of an olefin, *cis*-cyclooctene, in the RDE solution (Figure 4C) produced qualitatively similar results but with a somewhat smaller enhancement of currents at all rotation rates ($n_{app} = 2.2$) including those in the electrocatalytic region at low rotation rate. The change is small but implies that the reaction between olefin (present at large excess) and oxo complex is fast enough to be competitive with the rate of formation and transport of the oxo complex through the hydrodynamic diffusion layer. The significance of this observation is to open the way to increasing the catalytic efficiency observed for the electrolytic epoxidation based on manipulation of reaction rates and electrochemical mass transport. In general, it appears desirable that the mass transport away from the electrode be fairly rapid (to avoid the short-circuit reaction) but not so rapid as to prevent production of the doubly reduced $[Mn^{III}(salen)–O_2]^-$ complex.

Controlled-Potential Electrolysis. Controlled-potential electrolyses (CPE) were performed on stirred solutions to effect the epoxidations reported in Table I and also to ascertain the stability and efficiency of the Schiff-base catalyst. The electrolysis potential was maintained at −0.45 V vs SSCE, which according to the RDE results should achieve a steady-state limiting current. Figure 5 shows a typical current vs time plot during the electrolytic oxidation of cyclohexene; the current decays fairly rapidly over a period of about 15 min and gradually approaches a steady value that is about one-third of the initial current. The catalytic efficiencies reported in Table I are based on the integrals of these current time curves up to the time a sample of the solution is withdrawn for GLC analysis of its epoxide content.

The UV–vis spectrum of this solution was also monitored by periodic withdrawals with results given in Figure 6. The spectral data show a decrease in the quantity of catalyst present in solution with increasing time. After approximately 90 min the absorption band at 417 nm is about one-third the initial intensity; this result parallels that seen in the current–time data of Figure 5. The broad absorption centered around 756 nm may be associated with the decomposition product of the catalyst, but we have not tried to isolate or characterize this compound or compounds.

We have not attempted in this study to optimize the conditions for electrolytic epoxidation of olefins, but it is obvious that such an effort would have limited utility, since the $[Mn^{III}(salen)]^+$ catalyst has a limited lifetime. This behavior contrasts sharply with the manganese porphyrin system, which showed[5] little catalyst decomposition, <5%, after more than 6 h of reaction. The instability of the Schiff-base catalyst likely arises from the susceptibility of the imine linkage to oxidation by dioxygen or oxo complex. Further studies will be required to ascertain whether the Schiff-base catalyst can be stabilized toward oxidative decomposition by appropriate derivatization of the ligand.

Acknowledgment. This research was supported in part by a grant from the National Science Foundation (R.W.M.).

(24) F is Faraday constant, v is kinematic viscosity of the solvent, A is electrode area, D_0 is the diffusion coefficient, and C_0^* is the bulk concentration of the $[Mn^{III}(salen)]^+$ complex.

(25) The experimental Levich line (—) lies between the hypothetical lines for which two and four electrons would be passed per $[Mn^{III}(salen)]^+$.